Monitoring the Performance of a Residential Central Air Conditioner under Reduced Evaporator Air Flow on a Test Bench

Manivannan Palani, Research Assistant
Dr. Dennis O'Neal Ph. D., P.E.
Dr. Jeff Haberl Ph. D., P.E.

November 1992

DRAFT

ABSTRACT

This report presents results from degraded performance measurements of a residential air conditioning system operating under reduced evaporator air flow. Experiments were conducted using a R-22 three-ton split-type cooling system with a short-tube orifice expansion device. Results are presented here for a series of tests in which the air flow across evaporator was reduced by 25%, 50%, 75%, and 90% of normal amount of air flow as specified by ARI. Return air temperature was maintained at 80 F dry bulb for all the standard and degraded experiments. Experiments were conducted for three different return humidity conditions of 20% RH, 45% RH, and 65% RH and three outdoor conditions of 70°F, 85°F, and 100°F dry bulb temperature.

At present, very little information has been published which quantifies the degraded performance of a residential cooling system operating under reduced evaporator air flow. Degraded performance measurements can provide information which could help electric utilities evaluate the potential impact of system-wide maintenance programs.

TABLE OF CONTENTS

LIST OF FIGURES

LIST OF TABLES

NOMENCLATURE

C_p	Specific heat at constant pressure, Btu/lb ^oF
h	Enthalpy of fluid, Btu/lb.
m	Mass flow rate, lb./min
Q	Air flow rate, ft^3/min
T	Temperature, ^oF
v	Specific volume, ft^3/lb
w	Specific humidity, lbm/lba

Subscripts

a	air
c	condenser
e	evaporator
i	inlet
n	standard conditions
o	outlet
$\mathbf{o_d}$	outdoor
p	constant pressure
r	refrigerant
$\mathbf{r_a}$	return air
$\mathbf{s_a}$	supply conditions

GLOSSARY OF TERMS

ARI	Air Conditioning and Refrigeration Institute
ASHRAE	American Society of Heating, Refrigeration and Air Conditioning Engineers
Btu	British thermal unit
CFM	Cubic feet per minute
DBT	Dry Bulb Temperature
DOE	Department of Energy
EER	Energy Efficiency Ratio
floodback	Condition in which liquid enters the compressor
fpm	Feet per minute
HVAC	Heating Ventilating and Air Conditioning
lbm	Pounds mass
lbma	Pounds mass of dry air
NIST	National Institute of Standards and Technology
OD	Outer diameter
O.D.	Outdoor
ORNL	Oak Ridge National Laboratory
RH	Relative Humidity
SHR	Sensible Heat Ratio (sensible cooling load / latent cooling load)
Subcooling	the difference between refrigerant saturation temperature and the measured temperature at the outlet of condenser
Superheat	the difference between refrigerant saturation temperature and the measured temperature at the inlet of compressor
WBT	Wet bulb temperature

CHAPTER I

INTRODUCTION

Outline of Introduction

The impact of air conditioners on electricity consumption in national level and in Texas is reviewed in this chapter. From the assessment of the current field installation practices it appears that significant amounts of air conditioners are operating under degraded conditions. There are also constraints on providing periodic service which could help to maintain the original efficiency of the air conditioners. A brief discussion of currently emerging monitoring technologies is also done here. The primary motive behind current investigation is outlined in objective section.

Overview of Air Conditioners Use in U.S.

In the year 1987, the electricity consumption in U.S. by end-use was, Residential sector 35%, Commercial sector 27%, and Industrial sector 35% (Energy Information Administration [EIA], 1991). Heating and cooling systems consume 27% of the electricity used in the residential sector. The average annual residential electricity cost was 685$ (EIA, 1989). It is important to pay attention on electricity cost because, in the last 15 years the residential electricity cost was increased by 200% (Energy prices, 1991). Due to lack of awareness customers are unwilling to pay for the conservation. Also implementing the conservation is also difficult because of the diffuse pattern of use of electricity by air conditioners. It was estimated that atleast 30.7 million central system air conditioners are used in the U.S. residences (EIA, 1989).

Assessment of the Need for the Service

Field studies show that many of the existing installations are of poor quality and require immediate service to save the equipment or to restore it to rated efficiency (Neal, 1987; Proctor, 1991). Experts from air conditioning service industry also point out that manufacturers are not addressing the difficulties that arise in field installations (Wheeler, 1991). From the field studies, Proctor found that the HVAC contractors who are responsible for maintaining air conditioners

U.S. Electricity End-Use, 1987
(850 Billion kWh)

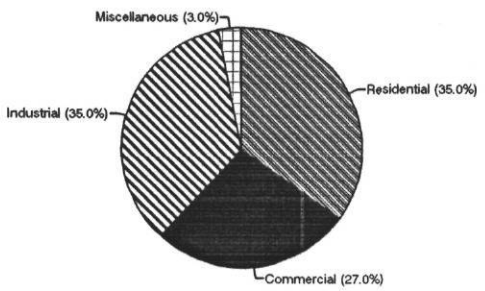

U.S. Household Electricity
End-Use 1987

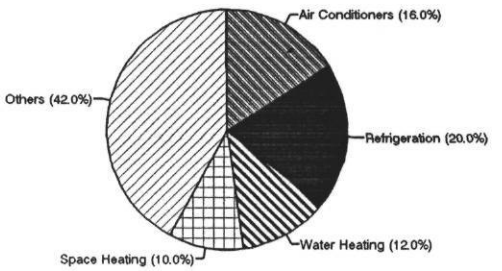

Household Energy Consumption and Expenditures 1987
(Energy Information Administration)

Texas Electricity End-Use, 1987
(76.5 Billion kWh)

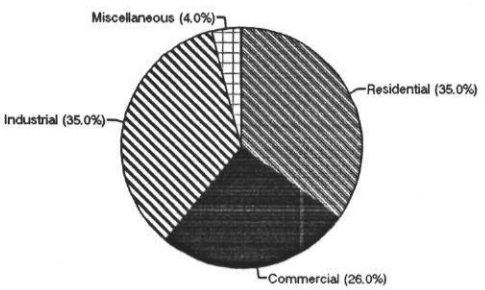

Texas Household Electricity Use
End-Use 1987

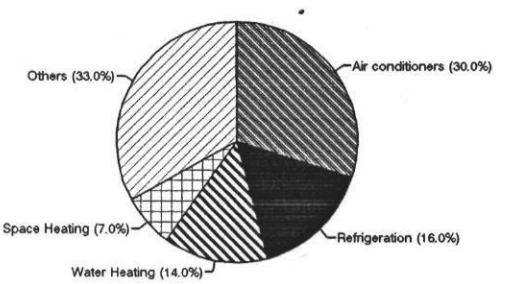

PUCT End-Use Modeling Project
(Public Utility Commission of Texas, PUCT)

were not identifying or solving the problems that led to high energy bills (Proctor, 1991). Neal also expressed the same opinion after conducting a field installation survey in North Carolina (Neal, 1987).

The following list of prevalent field degradations can serve as a yardstick to assess this problem;

Reduced air flow: 67% (Proctor), 30% (Neal), 17% (Hewett)

Undercharging or overcharging: 53% (Proctor), 70% (Neal), 72% (Hewett)

Refrigerant leaks and kinked lines 40% (Proctor).

Constraints on Periodic Service

Current trends in the residential air conditioning service industry are based primarily on corrective maintenance procedures which are initiated only after a failure occurs. While preventive maintenance can help maintain optimum system performance, some possible reasons include: (1) customers' reluctance to pay the price for regular check-ups, and (2) contractors' lack of the necessary knowledge to provide an effective preventive maintenance procedure.

Preventive maintenance can be primarily classified as (Anderson, 1990): (1) On Condition Maintenance (OCM) where degradation prior to functional failure can be detected by periodic inspections and evaluations, or (2) Condition Monitoring (CM) where degradation prior to functional failure can be detected in sufficient time by instrumentation(e.g., measuring temperatures or pressures).

Regardless of which approach is followed preventive maintenance is only effective when potential failures can be ascertained reliably and inexpensively and where the prevention of the failure more than pays for the diagnostics. Current preventive maintenance technology is yet to attain this position, because from field measurements, Hewett found that for small capacity units tune-ups are not cost-effective to the utility (Hewett, 1992).

Appearance of New Monitoring Units

One of the major problems facing the residential cooling service industry is a lack of adequately trained service technicians (Silver, 1989). The currently available service techniques are based on the field experience of the service personnel and remedial measures vary widely with each individual's background. Recently Environmental Protection Agency (EPA) mandated a rule which demands the technicians to recover and recycle the refrigerants and it also recommends that standardizing the training program received by refrigerant technicians (Mahoney, 1992). Automatic monitoring and diagnostic systems based on the air conditioning theory could address the need of the air conditioning industry in such areas as 1. to develop a standardized service procedure and 2. to asses the cost-effectiveness of the service.

Some commercially available automatic diagnostic systems are already beginning to appear. Kaler developed one such monitoring device which continuously monitors the HVAC system for selected system malfunctions (Kaler, 1990). This device continuously tracks the temperatures of an HVAC system and evaluates this value with an embedded knowledge base, and warns the owner in advance of any potential trouble.

"CoolGuard" developed by Dencor Inc., is an electronic monitoring device that can detect failure symptoms (Coolguard, 1992). It monitors return and supply air temperature and outdoor air temperature for abnormal values. Remote monitoring possibility is also available with this system.

Foster of Whitbread (U.K.) discuss a computerized monitoring and pre-failure diagnostic system for low to medium cost refrigeration equipment (Foster, 1992). Whitbread R&D engineers closely studied the performance of wide range of refrigeration equipment's used in restaurants and pubs and developed a patented technique which can learn correct operating characteristics. It then monitors the units to detect abnormal operating conditions.

It appears that current monitoring technologies are not matured sufficiently, because from the field studies conducted to evaluate two automatic monitoring and diagnostic devices it was found

that their performance were not satisfactory in the field installations (S. Englander, personal communication, September 27, 1991). Lack of the theory on residential air conditioning monitoring is the primary cause for hindering the further implementation of these devices.

Overview of Air Conditioners Use in Texas

Texas consumes nearly 9% of the electricity used in U.S. Electricity consumption in Texas by end-use can be given as, residential sector 35%, commercial sector 26%, and industrial sector 35%. Approximately 5.9 million single-family dwelling residences are in Texas and 70% of them have central space cooling systems. By 1998, 80% of the Texas households are expected to have central cooling systems. The most commonly sized central air conditioners have three tons of cooling capacity and the average SEER for the existing units is 8 Btu/watt-Hour. The average SEER value for the new units is 10 Btu/watt-Hour (PUCT, June 1990).

Impact of Air Conditioners Energy Use on Utilities

In Texas, central air conditioners consume nearly 30% of the residential electricity use. This quantity is expected to remain unchanged till 1998. The influence of air conditioners on the residential peak load is very high (90%) and the two third of the commercial peak load is due to air conditioners (Zarnikau, 1992; Reddy, 1992).

Significant amount of cooling energy consumption can be saved by improving the efficiency of the air conditioners (Zarnikau, 1992). The demand side management (DSM) program promoted by utilities around the nation gives incentive to customers to buy high efficiency air conditioners which can pass the Appliance Minimum Efficiency Standards, which became effective in 1992 (United States, 1987). Utilities are also being asked to increase and measure their demand-side savings. It was estimated that 973 million kWh of electricity should be saved in 1999 because of the National Appliance Efficiency Standards and the peak demand savings should be 600 MW by 1999, in Texas. However, a high efficiency air conditioner will only reduce energy use if it is installed and maintained properly.

Objective of Current Investigation

Currently, very little information is available which describes the performance of air conditioners under degraded conditions. The air conditioning industry has shown a concern and several trade journal articles address this issue (Neal, 1986; Rutkowski, 1990). This problem is further compounded by a lack of consensus for developing proper service procedures (Powell, 1988).

A detailed discussion of performance which has been observed on a test bench is presented in this report. The primary focus of this report is to investigate the performance of an air conditioner under reduced evaporator air flow. Reduced evaporator air flow is caused by; 1. A dirty filter or a dirty coil, 2. The duct blockage, and 3. A loose belt or pulley (in the case of belt driven blowers). Evaporator air flow was reduced by 25% to 90% of normal amount of air flow. Performance was monitored by varying return air humidity and outdoor dry bulb temperature.

The final objective of quantifying the measured degraded performance is presented in this report in the following fashion; (a.) the review of previous work, (b.) experimental apparatus and procedure, (c.) data reduction and performance calculations, (d.) results and discussion, (e.) summary and conclusions. The long term goal of this work is to classify and simulate degraded conditions for the most widely experienced problems on a test bench so that eventually the field procedures developed which are capable of recognizing the degraded conditions.

CHAPTER II

REVIEW OF PREVIOUS WORK

Outline of Previous Work

The review of previous work is organized in two groups, namely: 1. Failure patterns and field measurements, 2. Degradation studies. Discussions on failure patterns and field measurements are necessary to review the current situation and to set a general guideline for further work required to improve the efficiency of the air conditioners. Degradation studies, which are discussed here are mostly conducted in a laboratory atmosphere and they attempts to quantify the effect of degradation on efficiency.

Failure Patterns and Field Measurements

Among the five literatures reviewed under failure patterns and field measurements, Karger (Karger, 1984) and Lewis (Lewis, 1987) discuss the component wise failure rates of an air conditioner. Neal (Neal, 1987), Proctor (Proctor, 1991), and Hewett (Hewett, 1992) made field measurements to access the quality of installation and degradation in efficiency.

Karger and Carpenter discussed failure patterns of residential air conditioning units based on their survey of 531 failed units. This is one of the first studies conducted on failed air conditioning systems. Their study indicated that failure rates for electrical controls and miscellaneous electrical devices was the most prevalent at 31.4% of the total number of failures, followed by refrigerant leaks 17.2%, compressors was 13.5% and outdoor fans at 11.5%.

Lewis surveyed 492 large HVAC dealers to compile information on heat pump service life. He discovered that refrigerant leaks were the major cause for failure, totaling 19% of failed units, followed by compressor motor circuits were 16%, and mechanical part failures were 12%.

Neal investigated the quality of residential air conditioning system installation and service in North Carolina. His random survey of 10 units indicated that inadequate evaporator air flow was present in 3 of the 10 units(30%) and improper charging was in 7 units(70%). He concluded that

a very high percentage of air conditioning units have installation or service problems that affect homeowner's energy bills and comfort.

Proctor tested fifteen homes in Fresno, CA which reported very high summertime energy consumption in PG&E's Appliance Doctor Pilot Program, a project designed to investigate the causes for the high energy bills. Proctor's results showed low evaporator air supply existed in 10 out of 15 sites(67%). Overcharging and undercharging was found in 8 locations(53%). Refrigerant leaks and kinked lines were present in 6 houses(40%). Remedial measures reduced cooling energy costs from 10 to 30%. He concluded through interviews and field tests that the HVAC contractors who maintained these systems were not identifying or solving the problems that led to high energy bills.

Hewett et al., sought to quantify the energy and demand savings through efficiency tune-ups of commercial unitary cooling equipment in the service territory of a major New England utility. They tuned up and monitored 18 systems (7 dual compressor systems) which range between 4 to 15 tons cooling capacity. Their results show that reduced evaporator air flow condition exist in 3 units(17%), overcharging was found in 10 units (60%) and undercharging was found in 8 units (40%). They also found that none of the thermostatic expansion valves(13 systems) provided correct superheat. They conclude that "tune-ups do not appear to be cost-effective to the utility except perhaps for larger equipment". Efficiency tune-ups resulted in an average energy savings of 9 to 10%.

Degradation Studies

Houcek (Houcek, 1984) and Farzad (Farzad, 1988) conducted degradation experiments to quantify the effect of undercharging and overcharging on efficiency. Currently, very little information is available to predict the degradation in efficiency due to reduced evaporator air flow and reduced condenser air flow.

Houcek studied the effect of improper charging by conducting experiments on a 2-ton split system with 37 feet of interconnecting refrigerant lines. In his experiments supply air entering the

indoor coil was maintained at 80°F DBT and 67°F WBT. Air entering the outdoor unit was maintained at four different conditions: 70°F, 82°F, 95°F and 100°F. Houcek's experiments showed that at 95°F outdoor conditions, overcharging by 23% decreases the operating cost by only 0.5%. However, this was observed to cause a floodback condition (Floodback describes a situation when liquid refrigerant enters the compressor. Compression of liquid refrigerant will cause mechanical failure of the compressor). For undercharging, it was estimated that the operating cost increased by as much as 52%. He recommended a new device (a Visual Accumulator-Charger) for charging air conditioners effectively.

Farzad studied the effect of undercharging and overcharging for three expansion devices: (i) a capillary tube, (ii) a short-tube orifice, and (iii) a thermostatic expansion valve. He conducted his experiments under controlled conditions specified by DOE/ARI testing procedures for Unitary Air Conditioners. He varied the system charge from -20% to +20% for different outdoor temperatures. His study showed that capillary tube expansion is more sensitive to off-charge conditions than other types of expansion valves. For a 20% undercharge the Seasonal Energy Efficiency Ratio (SEER) was reduced by 20%, while overcharging by 20% produced an 11% reduction in SEER. He found that the SEER was not very sensitive to changes from -20% to +20% of the correct charge when an orifice tube is used for an expansion device.

Summary of Review of Previous Work

From the review of failure patterns and field measurements we can conclude that (i) Significant number of air conditioners are working under degraded conditions, (ii) Current installation and service techniques are not satisfactory. Also from degraded studies, we learned that it is possible to quantify the amount of degradation. This information could be useful to assess the cost effectiveness of air conditioner tune-up. A summary of work done by various authors and the products available in the air conditioning service field is listed in Table 2.1. By reviewing Table 2.1., and excluding few large air conditioners manufacturers, we can conclude that,

Authors	Unit failure rate survey	Field performance check	Degraded Experiments	Field Monitoring system	Remote Diagnostics	Service Support	Service Procedure
Karger	* (A/C)						
Lewis	*(Heat pump)						
Neal		*					*
Proctor		*					
Hewett		*					
Houcek			*				
Farzad			*				
Kaler				*			
Dencor				*	*		
Foster				*			
Wheeler							*

Table 2-1. Index of authors and products

1. Currently very little information has been published which encompass the whole range of air conditioning service activities

2. Lack of comprehensive theoretical and experimental investigation is available to explain and detect the degraded conditions.

3. Further work is required to effectively utilize some of the state-of-the-art technologies of electronics for the purpose of monitoring and diagnostics.

From the above arguments it is imperative that the air conditioning diagnostics should be explored from first principles so that they can be carried out successfully to save energy and resources.

CHAPTER III

EXPERIMENTAL APPARATUS AND PROCEDURE

Outline of Experimental Apparatus and Procedure

This chapter describes the background of experimental apparatus and procedure for conducting the degraded tests. Experimental apparatus was mounted on a split test bench as separate indoor and outdoor sections which facilitate them to locate in the indoor and outdoor rooms of Psychrometric chambers. Description of sensors and the location of measurements are discussed in the measurement section. Calibration of instruments is discussed in the calibration section. The Procedures section describes the tests conducted in the room atmosphere and in the Psychrometric chambers.

Description of Test Bench

In this project, the air conditioning system considered for analysis is a standard split system unitary air conditioner with a hermetically sealed reciprocating compressor. The cooling coil has a maximum three ton capacity. A short-tube orifice was employed as expansion device. The refrigerant flow path and the air flow path are shown schematically in Figure 3.1. A detailed arrangement of components on the test bench is shown in Figure 3.2. The technical specification for each component is given in Table 3.1.

Indoor Section

The arrangement of indoor test section included a removable flow restrictor, a centrifugal type blower and a cooling coil (vertical type evaporator). An air flow restrictor (pre-drilled plywood board) was placed at the entrance of the indoor air flow chamber to simulate the reduced evaporator air flow conditions. The supply air which was passed across the cooling coil was routed back in to the indoor room after leaving the indoor chamber.

Outdoor Section

The outdoor test section consisted of, a reciprocating compressor, a spine-fin condenser coil and a propeller type outdoor fan. The outdoor fan was mounted on the top of the condensing coil. The conditioned outdoor room air is inducted across the condensing coil and discharged above in to the room.

Measurement

A list of properties which were measured at the test bench is shown in Table 3.2. A total of 21 quantities was measured with a data acquisition system. Refrigerant pressures and temperatures were measured at six locations, as shown in Figure 3.2. Refrigerant temperatures were measured with thermocouple probes which were installed in the refrigerant lines. The thermocouple probes were mounted parallel to the flow in the tubes to minimize conduction errors. Copper-Constantan thermocouples were used to measure both refrigerant and air temperatures.

Properties measured on the air side included dry bulb temperature and relative humidity at outdoor conditions and supply conditions. Return air dry bulb temperature was measured by a 16-element thermocouple grid before it entered the coil. Two flow straighteners were installed before and after the cooling coil to maintain a uniform air flow across the cooling coil. Supply air temperature was measured with another 16-element thermocouple grid before it enters the flow measurement chamber. Return and supply humidity sensors were located near the inlet and outlet thermocouple grids. The outdoor fan, air discharge temperature was measured by a 16-element thermocouple grid which was placed above the condenser fan.

The refrigerant mass flow rate was measured at the liquid line before the expansion valve. The refrigerant mass flow was measured with two Coriolis-effect (Macken) mass flow meters mounted in parallel. The pressure drop across the mass flow sensors was below 12 psig which is the allowable upper limit by ASHRAE Standard 116-83 (ASHRAE, 1983).

The amount of supply air was measured by an Air Movement and Control Association (No. 210) flow chamber. This chamber contained four ASME nozzles, an 8-inch, two 5-inch, and a 3-inch diameter. The 8-inch diameter nozzle was used to measure the standard test (1150-1200

LOCATION	QUANTITY	UNITS	INSTRUMENT	RANGE AND TYPE	ACCURACY
1 Discharge line	Pressure	PSIG	Pressure Transducer	0 - 500 PSIG	+ - 0.5%
2 Liquid line	Pressure	PSIG	Pressure Transducer	0 - 300 PSIG	+ - 0.5%
3 Before expansion	Pressure	PSIG	Pressure Transducer	0 - 300 PSIG	+ - 0.5%
4 After expansion	Pressure	PSIG	Pressure Transducer	0 - 300 PSIG	+ - 0.5%
5 Evaporator outlet	Pressure	PSIG	Pressure Transducer	0 - 300 PSIG	+ - 0.5%
6 Compressor inlet	Pressure	PSIG	Pressure Transducer	0 - 300 PSIG	+ - 0.5%
7 Discharge line	Temperature	DEG F	Thermocouple	TYPE T (Copper -Constantan)	+ - 0.5 DEG F
8 Liquid line	Temperature	DEG F	Thermocouple	TYPE T (Copper -Constantan)	+ - 0.5 DEG F
9 Before expansion	Temperature	DEG F	Thermocouple	TYPE T (Copper -Constantan)	+ - 0.5 DEG F
10 After expansion	Temperature	DEG F	Thermocouple	TYPE T (Copper -Constantan)	+ - 0.5 DEG F
11 Evaporator outlet	Temperature	DEG F	Thermocouple	TYPE T (Copper -Constantan)	+ - 0.5 DEG F
12 Compressor inlet	Temperature	DEG F	Thermocouple	TYPE T (Copper -Constantan)	+ - 0.5 DEG F
13 Liquid line	Ref. flow	lb/min	Mass flow meter	0 - 10 lb/min, Coriolis-type	+ - 0.1%
14 Return air (indoor)	Dry bulb	DEG F	Thermocouple grid	TYPE T (Copper -Constantan)	+ - 0.5 DEG F
15 Return air (indoor)	RH	%	RH sensor	Thin film capacitive element	+ - 2.0%
16 Supply air	Dry bulb	DEG F	Thermocouple grid	TYPE T (Copper -Constantan)	+ - 0.5 DEG F
17 Supply air	RH	%	RH sensor	Thin film capacitive element	+ - 2.0%
18 Outdoor	Dry bulb	DEG F	Thermocouple grid	TYPE T (Copper -Constantan)	+ - 0.5 DEG F
19 Condenser Discharge air	Dry bulb	DEG F	Thermocouple grid	TYPE T (Copper -Constantan)	+ - 0.5 DEG F
20 Nozzle	Air supply	CFM	Diff. pr. transducer	0 - 1 inch w.g.	+ - 0.1%
21 Power supply	Outdoor unit Power	Watts	Watt Transducer	0 - 4 kW, 4 - 20 mA output	+ - 0.1%

Table 3.2. List of measuring instruments

CFM) and the 25% reduced air flow test. The 5-inch nozzle was used to measure the 50% reduced air flow test. The very low air flow conditions during 75% (300 CFM) and 90% (120 CFM) reduced air flow tests were measured by the 3-inch diameter nozzle. A differential pressure transducer was used to measure the static pressure gain before the supply nozzle, which was converted into air flow rate according to the ANSI/ASHRAE Std 51-1985 (ASHRAE, 1985). This standard includes the effect of supply air wet bulb temperature and the barometric pressure. The compressor and the condenser fan, power consumptions were measured with a watt transducer.

Calibration

The pressure transducers were calibrated with a dead weight calibrator before and after conducting the experiments. The accuracy was within +- 0.5 psig. Thermocouples were calibrated using an isothermal liquid bath. The accuracy of thermocouple was found to be within +-0.2 F, therefore it was decided to use the temperature readings as it was measured.

Relative Humidity sensors calibration

Relative humidity sensors were calibrated following the guidelines of National Bureau of Standards (NBS) for calibrating the Relative humidity sensors (Bryant, 1992). During the calibration it was found that the RH sensor's measurement error was function of both temperature and the amount of moisture in the air(Figure 3.3). The error during the calibration was varied from 5% to 12% from the reference values (saturated salt solutions) provided by NBS (NBS, 1983). Also, the NBS standard predicts as much as +- 4% variation in RH values for the saturated salt solutions. The degradation of accuracy in readings were also noticed (Bryant, 1992). Therefore a post calibration of RH sensors was also done after conducting all the experiments. In Figure 3.3 the initial-calibration and post-calibration errors of the Return air RH sensor is plotted as a function of return air dry bulb temperature and humidity ratio. The RH measurements were corrected individually for each test after considering the temperature and the amount of moisture present in the air during that particular test (Figure 3.3).

Procedures

General

Degraded tests were conducted at both in the room atmosphere and in the Psychrometric rooms. Outdoor temperature and the return air humidity were varied during the tests conducted in the Psychrometric rooms. After reviewing the references cited in previous chapters, the following degraded tests which represent the majority of degraded field conditions were selected for the investigation. :

1. Reduced evaporator air flow
2. Insufficient condensing unit air flow
3. System undercharging and overcharging
4. Non-Condensable gases (such as air) in the system
5. Restrictions in the refrigerant lines.

A complete description of tests conducted in Psychrometric rooms is discussed in Psychrometric section and in Appendix (Table A.2) This report only discusses the effect of reduced evaporator air flow on the performance of an air conditioner.

Room Atmosphere

Initially the test bench was assembled in the laboratory space which is not climatically controlled. Preliminary tests were conducted in the room atmosphere (normal laboratory temperatures). The indoor and outdoor sections were placed nearly 10 feet apart. The temperature of air entering the indoor section (return air) and the condenser inlet air was same as the normal room temperatures (nearly 75 F). The return air humidity was ranged from 45% to 60% RH.

Psychrometric Rooms

The indoor and outdoor section of the split-type air conditioner was installed in the indoor and outdoor rooms of Psychrometric room facility at the Energy Systems Laboratory, Texas A&M University. The Psychrometric rooms were constructed and maintained according to the American Society of Heating Refrigeration and Air conditioning Engineers (ASHRAE)

specifications (ASHRAE Standard, 1983). The room dry bulb temperature and humidity could be maintained within +/- 0.5°F of the set point. The desired set points were maintained by a Texas Instruments PM-550 controller.

Degradation simulation

Reduction in evaporator air flow was simulated using a plywood restriction board to cover the supply air duct. The plywood board was pre-drilled at several places to allow air flow from 100 CFM to 1000 CFM. Supply air flow was varied by covering the appropriate holes.

The low humidity (20% RH) standard and degraded tests were conducted initially for the three outdoor temperatures (70°F, 85°F, 100°F). The medium humidity standard tests were conducted at these three different outdoor dry bulb temperatures followed by high humidity standard tests which were repeated at the same outdoor dry bulb temperatures. For each reduced evaporator air flow condition (25% reduction etc.), the return air was maintained at the medium humidity level (45% RH) and the outdoor temperature was varied. After conducting the three medium humidity tests, the indoor humidity was raised to (65%) high humidity and another series of three degraded tests was repeated at three outdoor dry bulb temperatures. The air flow was maintained constant during all the six degraded tests. After conducting all the six degraded tests at one particular amount of reduction in evaporator air flow, these six degraded tests were repeated for another amount of reduction in evaporator air flow until all the required degraded conditions were simulated [Table 3.3].

Summary of Experimental Apparatus and Procedures

It was relevant to discuss the apparatus and instruments used in this experiments in detail because the reader should be aware of the methodology of the investigation and be able to evaluate the results for his needs. An important conclusion arrived from conducting the degraded experiments is the measurement and the calibrations of the instruments are very important. In particular, a complete calibration of RH sensors is essential to calculate the air side cooling capacity accurately.

Outdoor Dry Bulb	Return RH		
	20%	45%	65%
70 F	1. Standard Test 2. 25% reduced air flow 3. 50% reduced air flow 4. 75% reduced air flow 5. 90% reduced air flow	16. Standard Test 17. 25% reduced air flow 18. 50% reduced air flow 19. 75% reduced air flow 20. 90% reduced air flow	31. Standard Test 32. 25% reduced air flow 33. 50% reduced air flow 34. 75% reduced air flow 35. 90% reduced air flow
85 F	6. Standard Test 7. 25% reduced air flow 8. 50% reduced air flow 9. 75% reduced air flow 10. 90% reduced air flow	21. Standard Test 22. 25% reduced air flow 23. 50% reduced air flow 24. 75% reduced air flow 25. 90% reduced air flow	36. Standard Test 37. 25% reduced air flow 38. 50% reduced air flow 39. 75% reduced air flow 40. 90% reduced air flow
100 F	11. Standard Test 12. 25% reduced air flow 13. 50% reduced air flow 14. 75% reduced air flow 15. 90% reduced air flow	26. Standard Test 27. 25% reduced air flow 28. 50% reduced air flow 29. 75% reduced air flow 30. 90% reduced air flow	41. Standard Test 42. 25% reduced air flow 43. 50% reduced air flow 44. 75% reduced air flow 45. 90% reduced air flow

Table 3.3. List of experiments conducted in Psychrometric room

CHAPTER IV

DATA REDUCTION AND PERFORMANCE CALCULATIONS

Outline of Data Reduction and Performance Calculations

The preliminary data reduction process is discussed in the raw data processing section. The test duration and the properties which are measured are illustrated graphically through the time series plots. Also, the time series plots are helpful in visualizing the dynamic conditions occurring at 90% reduced air flow tests. The air and refrigerant side capacity calculations are discussed in the performance calculations sections. Construction of Pressure-Enthalpy chart and Psychrometric chart is also included in this chapter.

Raw Data Processing

During each test, the refrigerant and air side properties were measured continuously at the interval of 15 seconds. The time series plots which were shown in Figures 4.1. and 4.2. describe the test operating conditions during a normal air flow test (standard) and a 90% reduced evaporator air flow test (degraded). The time series plots which were shown here, correspond to the medium humidity return air (45% RH) at 85 F outdoor dry bulb conditions. The refrigerant pressures and refrigerant temperatures which were measured at six locations on the refrigerant lines (Figure 4.1.) was shown in the top row. The air side dry bulb temperatures and relative humidities were shown in the left hand side of the middle row. The air flow across the evaporator was shown in the right hand side of the middle row. The total refrigerant mass flow rate and the outdoor unit power consumption were included in the last row.

The duration of the standard tests and the 25%, 50% and 75% reduced air flow tests were thirty minutes and the duration of the 90% reduced air flow tests were nearly two hours and thirty minutes. For the normal test the steady state values were reached within 10 minutes after the start-up. However during the 90% reduced evaporator air flow test, the symptoms of serious

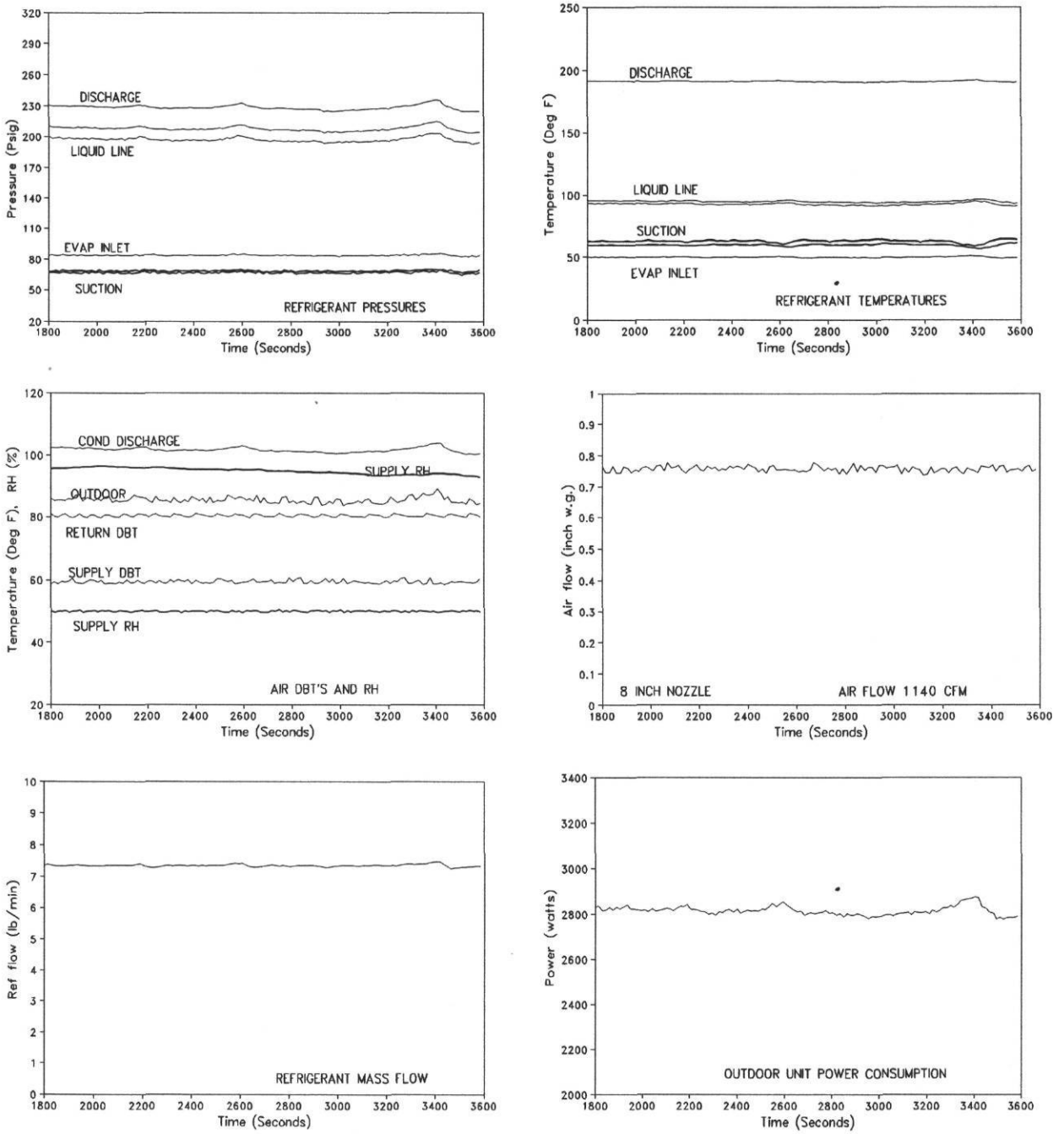

Figure 4.1. A sample time series plot for the standard test

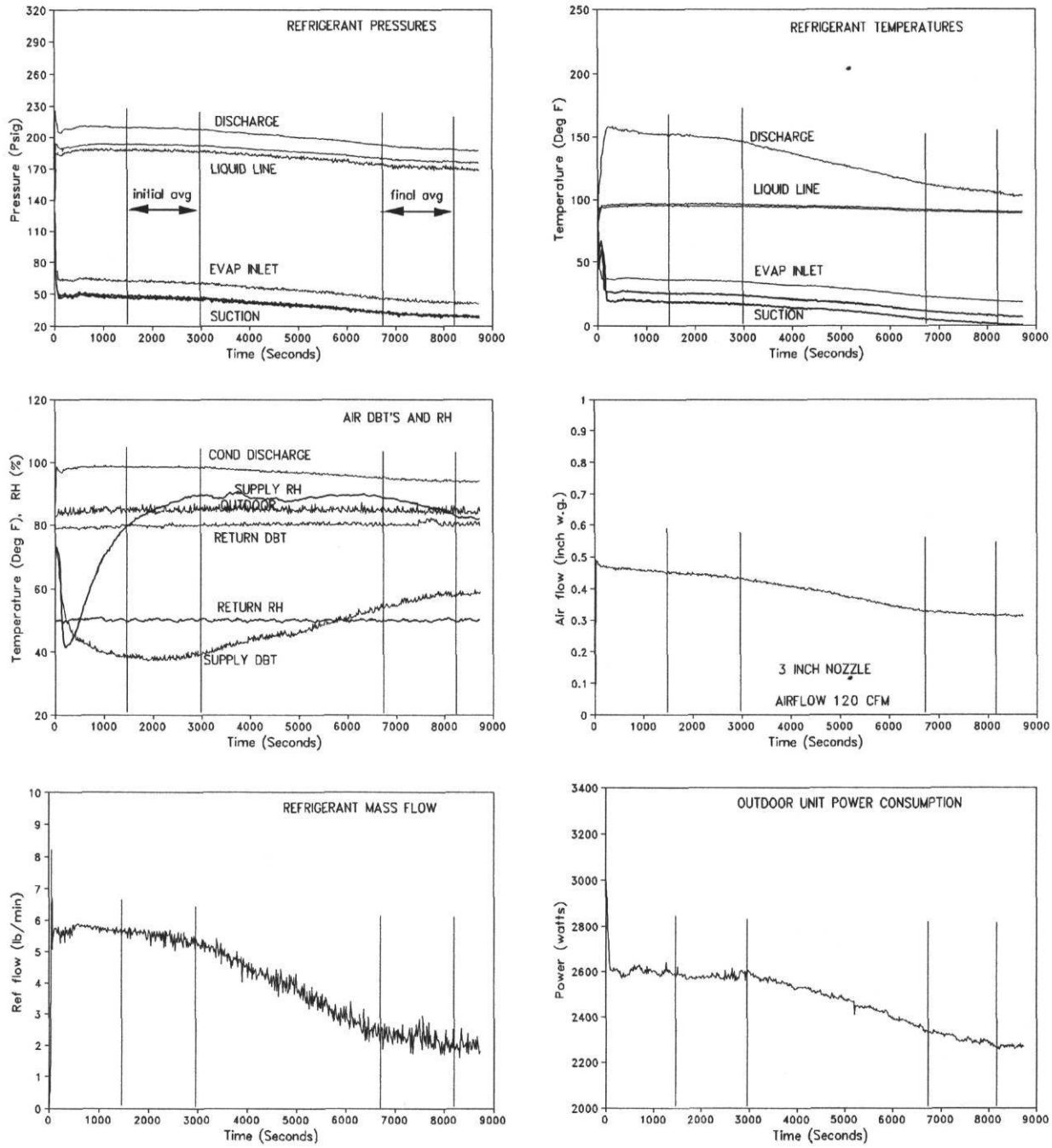

Figure 4.2. A sample time series plot for the 90% reduced evaporator air flow test

degraded conditions appeared only after 45 minutes from the start-up.

Refrigerant pressures and temperatures dropped to a very low value after an hour of reduced evaporator air flow operations. The supply air temperature started to rise after 45 minutes of the start-up and the supply air humidity also reached to a steady value during that period. The air flow across the evaporator was reduced by frost which was covering the evaporator coils. The reductions in refrigerant flow and the outdoor unit power consumption were also visible from the reduced evaporator air flow plots. Further discussions on this topic is included in the experimental observations sections in next chapter.

Return air temperatures were maintained at 80°F for most of the tests. However, return air temperature varied from 80°F to 77°F during 75% and 90% of reduced evaporator air flow. This was due to a slight amount of cold air re-circulation which occurred between the plywood restrictor and the cooling coil. This effects are similar to the thermal storage effects of the duct walls, and the non-uniform velocity and temperature distribution over the cross-section of the thermocouple grid as discussed by Tree et al., (Tree, 1981).

Performance Calculations

To calculate the performance factors, values measured during steady-state conditions were averaged for thirty minutes of the test. Refrigerant enthalpies at six locations were calculated using the refrigerant property calculation program developed by Kartsounes (Kartsounes, 1971). Air side enthalpy, specific humidity and specific volume were calculated by a Psychrometric program developed at the Energy Systems Laboratory, Texas A&M University[ESL].

Capacities were calculated for both refrigerant and air sides. Cooling capacity was calculated from air side enthalpy drop using the following equations,

$$\text{Sensible}, \quad Q_s = \frac{60 Q_a C_{pa} (T_{i,a} - T_{o,a})}{[v_{sa}(1+w_{sa})]} \qquad (4.1)$$

$$\text{Latent}, \quad Q_l = \frac{63600 Q_a C_{pa} (w_{i,a} - w_{o,a})}{[v_{sa}(1+w_{sa})]} \qquad (4.2)$$

Equations 4.1 and 4.2 can be combined as,

$$\text{Total,} \quad Q_t = \frac{60 Q_a (h_{i,a} - h_{o,a})}{[v_{sa}(1+w_{sa})]} \qquad (4.3)$$

where,

Q_a Supply air flow rate (CFM),

C_{pa} Specific heat at constant pressure for supply air (Btu/lb F),

$T_{i,a}$ Return air dry bulb temperature (F),

$T_{o,a}$ Supply air dry bulb temperature (F),

$w_{i,a}$ Return air humidity ratio (lbm/lba),

$w_{o,a}$ Supply air humidity ratio (lbm/lba),

$w_{s,a}$ Supply air humidity ratio (lbm/lba),

$v_{s,a}$ Supply air specific volume (ft^3/lbm),

$h_{i,a}$ Return air enthalpy (Btu/lbm),

$h_{o,a}$ Supply air enthalpy (Btu/lbm),

Need for Refrigerant Capacity Calculations

The cooling capacity and the energy efficiency ratio were calculated following ASHRAE guidelines as mentioned in previous sections. The operating test conditions during several of the reduced air flow tests were different (very low air flow rates and frost covered evaporator coils) from normally recommended conditions, and they are not covered in ASHRAE/ARI test procedures (ASHRAE, 1983). Because of lack of further information on this topic, it was difficult to evaluate the current findings with any other published scientific literature.

When the air flow across the evaporator was decreased, the subcooling at the outlet of condenser was decreased close to zero. The mass flow sensor used to measure the amount of refrigerant flow is accurate only in the region of single phase fluid. The presence of vapor at the inlet of flow sensor, even in a small quantity will decrease the reliability in the measurement of the refrigerant flow (Macken).

Therefore, the capacity calculations were made for both refrigerant and air side to improve the accuracy in calculations. Also it appeared that, it was necessary to describe the performance from both the refrigerant and air side to visualize the degradation when the air flow across the evaporator was reduced.

Refrigerant Capacity Calculations

Refrigerant capacity was calculated using:

Refrigerant capacity, $Q_r = m_r(h_{e,o} - h_{e,i})$ (4.4)

$h_{e,i}$ Refrigerant enthalpy at the inlet of evaporator (Btu/lbm),

$h_{e,o}$ Refrigerant enthalpy at the outlet of evaporator (Btu/lbm),

The inlet and outlet of evaporator in refrigerant lines are indicated as location '4' and '5' in Figure 3.1. As evaporator air flow was reduced there was considerable discrepancy existed between the air side and the refrigerant side capacity. A more elaborate discussion on this topic is given in the experimental section of the next chapter.

Refrigerant capacity corrections

As the air flow across the evaporator was reduced, the cooling load on the evaporator was decreased with a resulting decrease in the amount of superheat at the outlet of evaporator. From the Pressure-Enthalpy diagrams (Appendix A), we can see that the condition of refrigerant leaving the evaporator coil was a saturated mixture of liquid and vapor. Under these conditions the temperature measured at the outlet of evaporator was corresponding to the saturated pressure measured at that location or vice versa. Assuming saturated conditions at the outlet of evaporator will give error in estimating the refrigerant side capacity. To predict the exact state of refrigerant at the outlet of evaporator, we needed to know at least one more thermodynamic quantity at this location. Therefore, a compressor enthalpy balance was performed to predict the state of the refrigerant at the outlet of the evaporator. The compressor enthalpy balance can be given as,

$$m_r(h_{cout} - h_{cin}) + Q_{comp} = W_{comp} \times 3412 \quad (4.5)$$

where,

m_r, the refrigerant mass flow rate (lb/hr),

$h_{c,out}$ the enthalpy of refrigerant at compressor discharge,

$h_{c,in}$ the enthalpy of refrigerant entering the compressor,

Q_{comp} the amount of heat transferred from compressor to outdoor air or vice versa,

W_{in} power input to the compressor (kW),

neglecting the heat exchange between the compressor and the ambient air,

$$h_{cin} = h_{cout} - [(W_{comp} \times 3412) / m_r] \qquad (4.6)$$

The enthalpy at the outlet of compressor was calculated by the discharge pressure and temperature. By performing the above enthalpy balance we can calculate the quantity ($h_{c,in}$), the enthalpy of refrigerant entering the compressor shell. Neglecting the suction line heat loss, the enthalpy of refrigerant entering the compressor is equivalent to the enthalpy of refrigerant leaving the evaporator. Thus $h_{c,in}$ is equivalent to $h_{evap\ out,\ actual}$. This quantity $h_{evap\ out,\ actual}$ is illustrated in the Pressure-Enthalpy diagram at location 5 (Figure 4.3.) and used in equation 4.4 ($h_{evap\ out,\ actual} = h_{e,o}$) to calculate the refrigerant capacity.

The motor electrical and mechanical losses which occur in the compressor shell adds heat to the suction gas before it enters the compressor manifold. The conversion efficiency for electric motors which are normally used in the residential cooling environment is given as 0.85 to 0.89 [ORNL, NIST]. The mechanical efficiency due to friction is normally taken as 0.95 to 0.98. Therefore the heat added to suction gas in the compressor shell can be written as,

$$h_{c,\,in\,actual} = (h_{evapout,actual} + (W_{in} \times (1.0 - 0.85) \times (1.0 - 0.95))) \qquad (4.7)$$

This actual state of refrigerant at the beginning of the compression process(hc, in actual) is shown at location '6' in Figure 4.7.

Pressure-Enthalpy and Psychrometric charts

The Pressure-Enthalpy and Psychrometric charts were made by imposing the data points for the standard and degraded tests on the templates for these charts. Pressure-Enthalpy diagrams can be helpful to visualize the influence of various physical parameters on the vapor compression cycle (Figure 4.3). A complete list of Pressure-Enthalpy diagrams and the Pyschrometric charts for reduced evaporator air flow conditions are included in Appendix A.

Construction of Pressure-Enthalpy charts and Psychrometric charts

Initially, the standard and degraded tests are classified in to nine sections based on the return air humidity and the out door dry bulb temperature (Table 3.3.). Under each return air humidity and outdoor dry bulb temperature the refrigerant pressures and enthalpies corresponding to the salient locations of the vapor compression cycle are chosen (Figure 3.1). A skeleton line diagram was plotted by connecting the data points (data frame) in the Pressure-Enthalpy coordinate. This process is repeated for 1. Standard test, 2. 25% reduction, 3. 50% reduction, 4. 75% reduction and 5. 90% reduction in evaporator air flow. In few cases of degraded tests where the data quality was not satisfactory those data points were omitted from the plots. Finally, the data frame was imposed over the template of pressure-enthalpy chart.

Similarly, in the case of Psychrometric chart a data frame was made which illustrate the return air, supply air, condenser inlet and condenser outlet conditions. When the Pressure-enthalpy diagram and the Psychrometric chart for each section are ready they were combined together and plotted in a single page.

Utilization of Pressure-Enthalpy diagrams and Psychrometric charts

The primary purpose of plotting the standard and degraded test performance on the Pressure-Enthalpy diagram and the Psychrometric chart is to visualize the relative degradation of reduced air flow conditions. Specifically the following observations can be gathered from these charts.

1. The temperature drop due to pressure drop in the evaporator can easily be seen from the Pressure-Enthalpy diagram.

2. There is no significant drop in the refrigerant effect per pound of refrigerant up to 50% of reduced evaporator air flow.

3. The refrigerant quality at the outlet of evaporator decrease with decrease in evaporator air flow and liquid refrigerant starts entering the compressor.

4. A very low discharge temperature and increased pressure ratio for 90% reduction in evaporator air flow can be seen from the diagram.

5. The variation in refrigerant effect per pound of refrigerant flow with the outdoor temperature is clearly depicted.

6. The effect of outdoor temperature, return air humidity, and evaporator air flow on refrigerant superheat and subcooling can be recognized.

Similarly, the Psychrometric charts (Figure 4.3. and in Appendix A) can be helpful to visualize changes in return and supply air temperatures and the decrease in sensible heat ratio(SHR) which occurred under reduced evaporator air flow conditions.

Summary of Data Reduction and Performance Calculations

A representative illustration of the standard and degraded tests were made through time series plots. The dynamic nature of vapor compression cycle at very low air flow rates were described by Figure 4.2. (For further discussions, see experimental observations section in results and discussion).

The methodology of performance calculations and refrigerant capacity calculations were also described. Construction and utilization of Pressure-Enthalpy diagrams and Psychrometric charts can pave a way to open up new paradigms in HVAC, such as visualizing the performance through animation which is discussed by Haberl (Haberl, 1992).

Figure 4.3. An example Pressure-Enthalpy diagram and Psychrometric chart

CHAPTER V

RESULTS AND DISCUSSION

Outline of Results and Discussion

Results are presented in this report in three major groups: (1.) Summary of performance factors (Power, Cooling capacity, and EER), (2.) Temperature analysis, and (3.) Experimental observations. Also, a master summary of performance is prepared for the low, medium, and high return air humidity conditions (Tables 5.1, 5.2, and 5.3). In each summary table the following quantities are presented:

1. Return air temperature and relative humidity
2. Supply air temperature
3. Supply air temperature drop and condenser air temperature rise
4. Discharge and suction pressures
5. Discharge and suction temperatures
6. The amount of air flow across evaporator
7. The total electric demand
8. EER.

The performance under standard and degraded tests are presented in adjacent columns in the master summary table for easy comparison of the degradation in performance. The normalized degradation in performance due to the effect of reduced evaporator air flow has been summarized in Table 5.4. The summary of performance factors (Power, Capacity and EER) is described in Table 5.5. The Figures 5.1, 5.2, and 5.3 show the effect of reduced evaporator air flow on cooling capacity and EER. The temperature measurements are shown in Figures 5.5, 5.6, and 5.7. The Capacity and EER based on refrigerant side measurements are presented in the appendix (Table A.1).

SUMMARY OF PERFORMANCE FACTORS

Construction of Power, Cooling capacity and EER plots

Power, Cooling capacity and EER are the three necessary parameters to measure the performance of an air conditioning system. The above three quantities are referred in this report as performance factors. The performance parameters are presented in Figures 5.1 to 5.3 and in Tables 5.4 and 5.5.

In Figures 5.1 through 5.3 the normalized values of performance parameters are plotted against the evaporator air flow. Normalized values are calculated by dividing the performance parameters calculated under reduced evaporator air flow with the performance parameters calculated under normal amount of air flow rate. Thus,

$$\text{PER CENT (power)} = \frac{\text{Power (degraded test)}}{\text{Power (standard test)}}$$

Similarly,

$$\text{PER CENT (Cooling capacity)} = \frac{\text{Cooling capacity (degraded test)}}{\text{Cooling capacity (standard test)}}$$

$$\text{PER CENT (EER)} = \frac{\text{EER (degraded test)}}{\text{EER (standard test)}}$$

Performance plots are divided into three groups; (i) low humidity return air, (ii) medium humidity return air, and (iii) high humidity return air. Under each return air humidity condition there are three individual plots corresponding to the three outdoor temperatures. We can observe from Figures 5.1 through 5.3 that demand curves are linear in general under reduced evaporator air flow conditions. Cooling capacity and EER curves has a non-linear tendency above 50% reduced evaporator air flow conditions.

Discussion on Power, Cooling capacity and EER

The total power consumption included the compressor, blower and outdoor fan power. Compressor power consumption varied with return air humidity and outdoor temperature. The minimum demand for a standard test was during 70°F outdoor dry bulb at 45% return air

humidity. The maximum demand was during 100°F outdoor dry bulb at 65% return air humidity. The compressor power consumption during the dry coil tests at 70°F outdoor dry bulb was greater than the medium humidity test at the same outdoor temperature because of the high value of superheat (38°F) at medium humidity conditions which reduced the amount of refrigerant circulated and caused lower compressor power consumption.

Demand Reduction with Reduced Evaporator Air Flow

Results showed that as the evaporator air flow was reduced from the baseline value, the electricity demand, cooling capacity and EER were decreased. Power consumption decreased linearly, for all three return air humidity conditions (Figures 5.1, 5.2, and 5.3.). It was decreased by 5 to 10% for 25% reduction in evaporator air flow and 15 to 25% for 90% reduction in evaporator air flow. The slope of reduction in power consumption was larger in the case of dry coil than the medium humidity tests. As evaporator air flow was reduced, the reduction in blower power was larger than the reduction in compressor power under any return air humidity and outdoor temperature conditions (Figure 5.4.).

Reducing the evaporator air flow did not produce a significant decrease in the compressor input power. The reduction in compressor power was less than 10% up to 75 % reduction in evaporator air flow. At 90% reduced evaporator air flow, the reduction in total power consumption was varied from 15 to 20% (Figure 5.4).

The blower power consumption was calculated by using the normal values recommended by ASHRAE/ARI (365 watts/1000 CFM). The blower power consumption was typically around 15% to 20% of the compressor power consumption for the normal amount of air flow. In the case of reduced evaporator air flow, the blower power was derived through the fan efficiency curves applicable to forward curved fans (Madison, 1948). The blower power was decreased linearly up to 75% reductions in evaporator air flow. For 90% reduced air flow, the blower power reached a minimum value of 60 watts specified by the fan curves (Figure 5.4). The blower power was around 2.5% of the compressor power during the 90% reduced evaporator air flow conditions.

Figure 5.4. The variation in blower power and compressor power

		Low RH (20%)			Medium RH (45%)			High RH (65%)		
		Power	Capacity	EER	Power	Capacity	EER	Power	Capacity	EER
70 F Outdoor	Standard	0.00	0.00	0.00	0.00	0.00	0.00	0.00	0.00	0.00
	25% reduction	-9.59	-2.36	8.01	-2.46	-5.88	-3.51	-5.78	-18.89	-13.92
	50% reduction	-13.12	-22.37	-10.63	-6.98	-21.71	-15.83	-14.41	-21.04	-7.75
	75% reduction	-15.96	-44.74	-34.24	-10.47	-29.47	-21.22	-17.22	-38.63	-25.87
	90% reduction	-22.40	-72.81	-64.96	-15.56	-62.74	-55.87	-19.70	-77.34	-71.78
85 F Outdoor	Standard	0.00	0.00	0.00	0.00	0.00	0.00	0.00	0.00	0.00
	25% reduction	-6.37	-8.45	-2.22	-4.49	-7.13	-2.76	-5.43	-19.54	-14.91
	50% reduction	-11.05	-33.36	-25.08	-9.55	-24.58	-16.62	-12.94	-26.04	-15.05
	75% reduction	-14.90	-49.78	-40.99	-13.74	-40.71	-31.27	-16.12	-39.43	-27.80
	90% reduction	-24.98	-73.68	-64.92	-18.38	-67.19	-59.80	-21.94	-75.38	-68.46
100 F Outdoor	Standard	0.00	0.00	0.00	0.00	0.00	0.00	0.00	0.00	0.00
	25% reduction	-7.98	-11.08	-3.37	-3.66	-12.06	-8.72	-4.83	-23.53	-19.65
	50% reduction	-14.32	-37.58	-27.15	-11.18	-30.81	-22.10	-10.68	-30.02	-21.65
	75% reduction	-18.23	-55.26	-45.29	-13.23	-37.21	-27.63	-15.04	-37.08	-25.94
	90% reduction	-25.61	-75.78	-67.45	-20.09	-67.75	-59.64	-22.93	-67.82	-58.24

Table 4. Summary of reduction in performance (air side)

		Low RH (20%)			Medium RH (45%)			High RH (65%)		
		Power	Capacity	EER	Power	Capacity	EER	Power	Capacity	EER
70 F Outdoor	Standard	2970	30654	10.32	2807	31614	11.26	2982	38923	13.05
	25% reduction	2685	29932	11.15	2738	29755	10.87	2810	31571	11.24
	50% reduction	2580	23797	9.22	2611	24750	9.48	2552	30732	12.04
	75% reduction	2496	16939	6.79	2513	22297	8.87	2469	23887	9.68
	90% reduction	2305	8335	3.62	2370	11781	4.97	2395	8820	3.68
85 F Outdoor	Standard	3227	30108	9.33	3228	31013	9.61	3313	37935	11.45
	25% reduction	3021	27562	9.12	3083	28802	9.34	3133	30524	9.74
	50% reduction	2870	20064	6.99	2920	23391	8.01	2884	28057	9.73
	75% reduction	2746	15119	5.51	2784	18387	6.60	2779	22976	8.27
	90% reduction	2421	7924	3.27	2635	10175	3.86	2586	9341	3.61
100 F Outdoor	Standard	3605	28980	8.04	3577	30365	8.49	3685	36358	9.87
	25% reduction	3317	25769	7.77	3446	26703	7.75	3507	27803	7.93
	50% reduction	3089	18089	5.86	3177	21011	6.61	3292	25443	7.73
	75% reduction	2948	12965	4.40	3104	19066	6.14	3131	22878	7.31
	90% reduction	2682	7018	2.62	2858	9793	3.43	2840	11701	4.12

Low RH: Return 80 F DBT, 20% RH
Med RH: Return 80 F DBT, 45% RH
High RH: Return 80 F DBT, 65% RH

Power : Total power (Blower + OD Unit), Watts
Capacity: Air side capacity (BTUH)
EER : (Capacity / Power)

Table 5. Summary of electric demand, cooling capacity, and EER (air side)

Effect of Reduced Evaporator Air flow on Cooling Capacity

Cooling capacity was decreased linearly until about 50% evaporator air flow then began to drop sharply for the dry coil case (Figure 5.1.). For higher return air humidities, this phenomenon was delayed until the evaporator air flow was reduced by 75% (Figures 5.2. and 5.3). This drop in cooling capacity could be caused by two phenomenon: First, at very low air flow rates, the increase in specific volume and the reduction in volumetric efficiency decreased the refrigerant mass circulated across the evaporator. This reduced the refrigerant side capacity, which ultimately resulted in very low cooling capacity at air side. Second, at very low air flow rates the evaporator surface temperature reduced below freezing temperatures and frost formed on the surface of evaporator. The frost reduced the heat exchange across the evaporator. Another phenomenon relevant to reduced evaporator air flow condition is that the maximum amount of enthalpy that can be rejected by the supply air. Under normal operating conditions, the supply air enthalpy is reduced by 5.75 to 6.0 Btu/lb. In the case of 90% reduced air flow, supply air enthalpy drop was increased to three times the normal conditions. From the total enthalpy balance, it is evident that drastic reduction in cooling capacity will realize because of this limitation in heat exchange across the evaporator coil.

Effect of Reduced Evaporator Air Flow on EER

The reductions in the energy efficiency ratio (EER) were similar to reductions in cooling capacity (Figures 5.1.,5.2., and 5.3.). Performance was linear until about 50% reduction in evaporator air flow, and non-linear afterwards. The decrease in EER closely followed the decrease in capacity because the energy efficiency ratio was obtained by dividing the cooling capacity by the total power consumption. Reduction in EER was lower than that of capacity because the demand also decreased with reductions in air flow rate.

Effect of Return air Humidity on Capacity and EER

At the same outdoor temperature, the cooling capacity was increased with an increase in return air humidity. At low air flow condition this increase in cooling capacity due to increase in return air humidity was observed at all three outdoor temperatures (70°F, 85°F, and 100°F). At

each reduced air flow condition (for example at 50% reduced air flow rate) the degradation of dry coil and high humidity conditions were greater than medium humidity. Similarly, the above trend was exhibited for degradation of EER under reduced evaporator air flow conditions.

Effect of Outdoor Dry Bulb Temperature on Capacity and EER

Cooling capacity was reduced with increase in outdoor dry bulb temperature. This was primarily due to the reduction in refrigerating effect (refrigerant enthalpy drop at evaporator per pound of mass flow rate) with increase in outdoor temperature (Figure A.12). There was a slight increase in degradation of cooling capacity as outdoor temperature was increased. This trend was not significant in the case of medium and high humidity cases. The EER was decreased as outdoor temperature was increased, since the electric demand was increased and the cooling capacity was decreased with increase in outdoor temperature.

TEMPERATURE ANALYSIS

Temperature analysis was carried out to study the feasibility of predicting the performance by measuring the system temperatures at salient points. For preliminary analysis the following four temperature differences, are presented in Figures 5.5, 5.6, and 5.7.

1. Supply air temperature drop across evaporator
2. The air temperature rise across condenser
3. Refrigerant superheat at the suction line
4. Degree of subcooling at the liquid line.

These temperature differences are commonly used in the service industry to predict the degraded conditions.

Construction of Temperature Measurement Plots

The temperature measurement plots are classified in to three groups based on return air humidity conditions. The key temperature differences which are mentioned above are plotted against the amount of air flow across the evaporator. Under each return air humidity

classification the temperature measurements correspond to three outdoor temperatures are plotted. The uncertainty in the measurements is discussed in the temperature error limits section.

Temperature Error Limits

The temperature error limits are primarily based on the observations from the time series of properties measurement. The total number of reduced evaporator air flow tests conducted on the test bench was 45. Deriving an error limit based on all the 45 tests is not a satisfactory approach. Therefore the standard medium humidity test at 85 F outdoor temperature was selected as a representative test. From the time-series plots for this test, it was found that the return and supply temperature were varied by +- 2 F. Similarly for condenser it was +- 2 F. However the uncertainty in the case of condenser temperature rise was greater than evaporator temperature drop because, the range of evaporator temperature was almost twice than the condenser temperature rise. The subcooling error limit was based on weighing the variation in liquid line pressure (+-3 psig) and temperature both. The uncertainty in superheat stems from the variation in suction line pressure and temperature. The swing in suction temperature was dominant (+- 4 F) compared to suction pressure. There is no significant change in the measurements of pressures and temperatures between the standard test and the reduced air flow tests. Therefore the same error values are used between 10% of normal flow and 100% of normal flow.

Supply air temperature drop across the evaporator coil

Definition

Supply air temperature drop across the evaporator coil can be defined as,

Air temperature drop = (Return air temperature - Supply air temperature)

Supply air temperature drop across the evaporator is an important quantity to judge the amount of cooling available. The cooling capacity is a product of amount of air flow and the air side enthalpy drop per pound of air flow of the supply air. The corresponding energy relations are described in Equations 4.1, 4.2, and 4.3. From these equations, we can see that as supply air relative humidity was increased the drop in supply air temperature across the evaporator was

decreased and when the air flow across the evaporator was decreased the supply air temperature drop was increased.

Test Bench Results

The supply air temperature drop across the evaporator for three different return air humidity conditions is shown in Figures 5.6 to 5.8. The temperature drop across the evaporator for the standard test was 26°F at low humidity conditions (20% RH) to 14°F at 65% return air humidity conditions. As air flow was decreased the temperature drop increased non linearly for low relative humidity conditions (20%) and medium relative humidity conditions (45% RH). The increase in air temperature drop was nearly linear for 65% return air humidity conditions. Under all three return air humidity conditions and at different supply air flow rates, the temperature drop was more in the case of lower outdoor temperature (70°F) than 85°F and 100°F outdoor dry bulb. This was due to increased cooling capacity which occurred as outdoor dry bulb was lowered (Table 5.5 and Figure A-12).

Reducing the evaporator air supply increased the temperature drop across the cooling coil for all the three return air humidity conditions. However an increase in supply air temperature drop was highest in the case of dry coil where it was increased from 26°F at normal flow to 53°F at 10% of normal flow [Figure 5.5]. As return air humidity was increased the increase in supply air temperature drop across the cooling coil was reduced. This is due to increased latent load with increase in return air humidity. The sensible heat ratio (SHR) for low humidity conditions was nearly 1.0 for the normal amount of air flow and it was decreased to 0.85 when the air flow across the evaporator was reduced by 90%. For high humidity conditions the SHR was 0.57 for normal amount of air flow. When the air flow was decreased by 90% the SHR decreased to 0.47.

From the above discussions it is clear that, to measure the performance of an air conditioner under varying conditions (1. Normal or reduced amount of air flow across evaporator, 2. The amount of moisture in the return air, and 3. The out door dry bulb) we need to measure the amount of moisture in the supply air at inlet and out let of the evaporator.

Condenser discharge air temperature rise

Definition

The design air flow across the condenser is constant for residential air conditioners. However this quantity could decrease due to the accumulation of leaves, debris and various other materials which reduce the free surface available for air flow thus reducing the amount of air flow. The measurement of condenser discharge air temperature rise across the condenser plays an important role in traditional air conditioning service (Wheeler, 1989). The energy balance across the condenser is given as,

$$m_{a,od} X\ C_p\ (T_{ci} - T_{co}) = m_r\ (h_{ic} - h_{oc})$$

Where,

$m_{a,od}$ = Mass flow rate of air across condenser,

C_p = Specific heat of air,

T_{ci} = Condenser inlet air temperature,

T_{co} = Condenser outlet air temperature,

m_r = Mass flow rate of refrigerant,

h_{ic} = Enthalpy of refrigerant entering the condenser,

h_{oc} = Enthalpy of refrigerant leaving the condenser.

The above relation indicates that the air temperature rise across the condenser is directly proportional to the total heat rejected from refrigerant side. In turn, the total heat rejected from refrigerant side is basically a function of change in enthalpy and the amount of refrigerant circulated.

Test Bench Results

For the standard test the temperature rise across the condenser was 14°F. The temperature rise across the condenser decreased linearly up to 75% of reduced evaporator air flow conditions. Though the cooling capacity at evaporator was decreased non-linearly, the reduction in compressor capacity (i.e. compressor power consumption) was less than 10% (Figure 5.4) and the continuous accumulation of frost (thermal storage effect) at evaporator, which caused the

difference in behavior between the condenser capacity and the evaporator capacity (Condenser capacity is the total of evaporator capacity and the compressor power consumption).

Refrigerant superheat at suction

Definition

Superheat can be defined as the difference between the measured refrigerant temperature and the saturation temperature corresponding to the saturation pressure measured at the outlet of evaporator. The corresponding relation can be written as,

$$Superheat = (Tsat - Tsuction)$$

Where,

Tsat = Saturated refrigerant temperature corresponds to suction pressure,

Tsuction = Measured refrigerant temperature in the suction line.

It is necessary to maintain a certain amount of refrigerant superheat in the suction line to ensure a safe operating environment for the compressor. This minimum amount of superheat which is set at one particular indoor and outdoor conditions will vary throughout the cooling season. The degree of superheat also varies depending on the cooling load on the coil and the amount of refrigerant circulated. If the amount of refrigerant circulated is within design limits then a decrease in the cooling load will decrease the degree of superheat. When supply air flow across the evaporator is normal, the degree of superheat will vary depend the amount of refrigerant circulated. Overcharge conditions decrease the degree of superheat and undercharge conditions increase the degree of superheat.

Test Bench Results

The refrigerant charge admitted into the system was eight pounds which produced 12°F to 15°F superheat for 95°F outdoor, 80°F dry bulb and 67°F wet bulb return air conditions. As outdoor temperature was increased the superheat at suction decreased for the same amount of cooling load present at the evaporator coil. As air flow across evaporator was reduced the amount of superheat at suction reduced to zero. Under low humidity return air conditions and normal amount of air flow across the evaporator the superheat was zero at 100°F and 85°F

outdoor dry bulb temperatures. At 70°F outdoor dry bulb, superheat was around 10°F in the case of normal amount of air flow across evaporator. When the air flow was decreased below 50% of normal air flow superheat decreased to zero for all return air humidity conditions and outdoor temperatures. (Figures 5.5, 5.6, and 5.7, and also see P-H diagrams in Appendix A).

For medium humidity return air conditions (45% RH) the superheat for normal amount of air flow was 35°F, 20°F, 5°F corresponding to 70°F, 85°F, and 100°F outdoor dry bulb temperatures. The decrease in superheat was significant between 25% and 50% reduced air flow rate. At high return air humidity conditions the superheat was 40°F, 30°F and 20°F for 70°F, 85°F, and 100°F outdoor dry bulb temperatures. Above 50% reduction in evaporator air flow, the superheat was decreased to zero.

The superheat was increased with a decrease in the outdoor dry bulb temperature. Even though the refrigerating effect increased as outdoor temperature was decreased, the increase in superheat occurred because the refrigerant mass flow decreased with a reduction in outdoor temperature. An increase in return air humidity increased the superheat at the compressor suction which resulted from an increase in the cooling capacity.

Refrigerant subcooling at liquid line

Definition

Subcooling can be defined as the difference between refrigerant temperature and saturated refrigerant temperature corresponding to refrigerant pressure at the outlet of condenser. Thus the corresponding relation can be written as,

$$Subcooling = (Tref - Tsat)$$

Where,

Tref = Refrigerant temperature measured at the liquid line,

Tsat = Saturated refrigerant temperature corresponds to liquid line pressure.

The degree of subcooling will increase or decrease depending on the air flow across condenser and the amount of refrigerant circulated. Thus degree of subcooling is somewhat similar to degree of superheat in predicting the behavior of the system from the condenser side. Refrigerant

subcooling at the outlet of condenser was varied with outdoor dry bulb, the amount of air flow across evaporator, and the amount of moisture in the return air.

Test Bench Results

For low return air humidity conditions the subcooling was 9°F, 8°F, and 7°F for 70°F, 85°F, 100°F outdoor temperatures. For medium humidity and high humidity conditions it was slightly higher than the low humidity values. Subcooling was increased with decrease in outdoor dry bulb. As air flow was reduced subcooling decreased linearly.

A reduction in subcooling was observed with a reduction in the evaporator air flow rate. This reduction was caused by a decrease in liquid line pressure and a simultaneous increase in temperature as evaporator air flow was reduced (2 to 15 psig) at the same outdoor temperature. The decrease in liquid line pressure also reduced the refrigerant saturation temperature which reduced the temperature potential exist for subcooling (Figure 5.8). Another minor reason for the increased temperature (higher enthalpy) at the outlet of condenser was due to reduced refrigerant flow across condensing coil which resulted in change of flow patterns and temperature patterns which reduced the condensing heat transfer coefficient. Using the Oak-Ridge National Laboratories simulation model (ORNL, 1981), it was found that the overall heat transfer coefficient was reduced by 20% for the 75% reduced evaporator air flow rate.

Figure 5.8. The liquid line subcooling analysis

EXPERIMENTAL OBSERVATIONS

Description of 90% reduced evaporator air flow test

The enthalpy balance as it was described in Equation 4.3. is not applicable in the case of very low evaporator air flow rates, because a steady state was never achieved during very low evaporator air flow rates. Performance calculations were done at two intervals for 90% reduced air flow test. The initial average represents the conditions which were occurring in the first portion of the test. The final average represents the performance under severe degraded conditions. Performance data under both conditions were compared in Table 5.6. The initial average values are used in comparing the performance parameters and which is presented graphically in Figures 5.1 through 5.6 and in Tables 5.1 to 5.5. Exploring this phenomenon from the beginning of the 90% reduced evaporator air flow test will illustrate the dynamic situations which are occurring under the very low air flow situations.

(i) When the unit is switched on, the compressor circulates a finite amount of refrigerant which enters the evaporator as a cold two-phase mixture. In the evaporator a finite amount of cooling capacity is available from the refrigerant side but this capacity is not entirely transferred to air stream since the amount of air circulated across the evaporator was very low.

(ii) The amount of charge that was originally admitted into the system was based on the condition that only superheated vapor should enter the compressor. However due to insufficient load on the evaporator, not all the refrigerant which was passing through the evaporator was vaporized and a saturated two-phase mixture was drawn into the compressor.

(iii) The discharge temperature and pressure both reduced from the normal level.

(iv) The pressure at the outlet of expansion valve was reduced from the normal levels, which in turn decreased the temperature of the refrigerant entering the evaporator.

(v) The lower refrigerant temperature and the large air side enthalpy drop caused by the reduced evaporator flow conditions caused the formation of frost at the surface of the evaporator. The air side enthalpy drop per pound of airflow reached a near maximum value.

(vi) The processes, (ii) to (v) was continued when the air conditioner was on and the reduced air flow conditions were prevailing across the evaporator.

(vii) After 45 to 60 minutes the refrigerant temperature was found to be near 10°F. Evaporator was completely covered by the frost. Suction lines and the bottom of the compressor was covered with the frost. Refrigerant discharge temperature fell to a very low value and the supply air flow temperature drop was increased considerably (Tables 5.1, 5.2, and 5.3) .

(viii) The specific volume of refrigerant entering the compressor was increased by 30% of the normal case. The pressure ratio across compressor rose from 2.6 to 3.3. This increase in refrigerant specific volume and the increase in pressure ratio caused dramatic reductions in volumetric efficiency.

Volumetric efficiency

The volumetric efficiency was calculated by using the relation (ORNL, 1983),

$$\eta_{vol} = \frac{m_{r,\,actual}}{m_{r,\,ideal}} = \frac{m_{r,\,actual}\ \vartheta_{inlet}}{D\ S}$$

where,

$m_{r,\,actual}$ = measured amount of refrigerant mass flow rate,

υ_{inlet} = refrigerant specific volume at compressor shell inlet,

D = total compressor displacement (3.46 cubic inch),

S = rated compressor motor speed (3600 rpm).

Volumetric efficiency was reduced from 75% at standard conditions to 50% at 90% reduced air flow rate.

(ix) The amount of refrigerant flow was decreased by 50% of normal conditions. In extreme cases the refrigerant flow was decreased by as much as 80% of the normal flow. The very low evaporator temperature and the reduced pumping capacity of the compressor caused the refrigerant to accumulate in the evaporator and eventually decreased the amount of cooling capacity available from the refrigerant side.

(x) Air flow across the evaporator was further reduced by the frost

(xi) Further evidence for the above argument can be seen from Figure 4.2. and in Table 5.6, where the supply air temperature was increased after an hour of continuous operation.

(xii) From the above arguments we can conclude that the performance of an air conditioner under very low evaporator air flow conditions is a time dependent phenomenon.

Table 5.6. Dynamic behavior of 90% reduced evaporator air flow test

REVIEW OF CURRENT RESULTS AGAINST AVAILABLE LITERATURE

The effect of evaporator air flow tune-up

Test bench results indicated that as evaporator air flow was reduced the demand was also reduced at the cost of decrease in cooling capacity and efficiency. Proctor discuss this topic in Appliance doctor program that,

Increasing the air flow of an air conditioner improves the efficiency of the unit and increase the CRI (continuous running input). CRI is the kW input to the air conditioner when it runs without cycling. The CRI increases because cleaning the coil increases the load on both the inside fan and the compressor. Repairing a low flow condition (dry coil CFM/ton < 375) is estimated to raise the CRI by an average of 5%.

-John Proctor, Appliance Doctor Program, 1991, Page 33.

FUTURE DIRECTIONS

The preliminary results from the first phase of this on-going project are encouraging. Experience with degraded tests can provide a better procedure to simulate faults in the future. The ultimate goal of this project is to develop a temperature based diagnosis procedure. Experience with preliminary tests indicated that easily identifiable temperature patterns exist for each degraded condition which can be utilized for developing an automated diagnosis procedure (Figures 4.5, 4.6, and 4.7).

Some commercially available automatic diagnostic systems are already beginning to appear. Kaler developed one such monitoring device which continuously monitors the HVAC system for selected system malfunctions [43]. This device continuously tracks the temperatures of an HVAC system and evaluates this value with an embedded knowledge base, and warns the owner in advance of any potential trouble.

"CoolGuard" developed by Dencor Inc., is an electronic monitoring device that can detect failure symptoms [44]. It monitors return and supply air temperature and outdoor air temperature for abnormal values. Remote monitoring possibility is also available with this system.

"Fluke 52" a digital recording thermometer developed by Fluke Inc. can record minimum and maximum values of a set point in the system, or minimum and maximum values of the temperature difference between two points [42]. Measurements over time (subcooling or superheating) can be recorded using this instrument. Further testing of such systems on a test bench can accelerate their acceptance into the marketplace.

Danfoss-EMC Inc., markets NC-25, a compressor rack control system for supermarket refrigeration racks [45]. As large percentage of energy consumed in supermarket environment is due to refrigeration compressors, the NC-25 system optimizes compressor pressure for saving energy and to maintain trouble free operation. Danfoss also provides remote service through a

central monitoring center. Utilities can similarly provide a central service system for residential air conditioners by measuring temperatures.

Foster of Whitbread (U.K.) discuss a computerized monitoring and pre-failure diagnostic system for low to medium cost refrigeration equipment[46]. Whitbread R&D engineers closely studied the performance of wide range of refrigeration equipment's used in restaurants and pubs and developed a patented technique which can learn correct operating characteristics. It then monitors the units to detect abnormal operating conditions.

ACKNOWLEDGMENTS

This work was funded through the Texas A&M Energy Systems Laboratory Research Consortium.

CHAPTER VI

SUMMARY AND CONCLUSIONS

SUMMARY

1. Significant amount of savings can be achieved by providing a proper service to air conditioners. Current monitoring technologies have not achieved a satisfactory level yet but there is a potential exist to improve them for the purpose of preventive maintenance and to standardize the diagnostics procedure.

2. Review of previous work indicate that considerable amount of degraded air conditioners are in service, also there is a limited amount of information available in the area of quantifying the degradation.

3. A three-ton cooling capacity split system was mounted on a test bench for experimental investigation. The calibration and measurement sections are discussed in detail because they play a crucial role in obtaining the accurate data.

4. Performance under reduced evaporator air flow conditions of an air conditioner was measured by varying the the amount of air flow across evaporator 25%, 50%, 75%, and 90% of normal amount of air flow.

5. Performance was monitored under three levels of return air humidities, Low (20%), Medium (45%), and High (65%) and at three outdoor temperatures 70 F, 85 F, and 100 F.

6. It was difficult to obtain a steady value for the refrigerant mass flow rate at very low evaporator air flow conditions. The uncertainty in the measurement of relative humidity was also significant (+- 5%) at reduced air flow conditions.

7. Beside air side capacity calculations refrigerant side capacity calculations is also made to provide a comprehensive picture of degradation in performance.

8. A methodology was described in refrigerant side capacity calculations section to calculate the refrigerant side capacity when the quality of the refrigerant leaving the evaporator is a saturated mixture.

9. The Pressure-Enthalpy diagrams and Psychrometric charts were helpful in illustrating the effect of reduced evaporator air flow on the performance of an air conditioner.

10. The effect of outdoor temperature was more influencing than the return air humidity on the vapor compression cycle (Figure A.12). The predominant effect of return air humidity was, increased evaporator cooling load and higher discharge temperatures (Figure A.11). The compressor power was varied with the return air humidity and the outdoor temperature.

11. Test bench results are summarized in three sections; (1.) Master summary tables (Tables 5.1. to 5.3), (2.) Summary of Power, Capacity, and EER (Tables 5.4 and 5.5), and (3.) Temperature measurements (Table A-2). Refrigerant side performance is included in the Appendix (Table A-1.).

12. Demand reduction was linear under all return air humidity and out door temperature levels.

13. Cooling capacity and EER decrease linearly up to 50% reduced air flow rate. Air flow reductions above 50% of normal amount of cooling capacity and EER decrease non-linearly.

14. At 90% reduced evaporator air flow rate, the total power consumption was decreased by 15% to 20% and the EER was decreased by 65% to 71%. The degraded condition test results indicated that to maintain sufficient cooling, one definitely must have at least 50% of rated air flow.

15. At 90% reduced evaporator air flow conditions cooling cycle failed to achieve steady state even after considerable amount of period (1 hour). Frosting due to low evaporator temperature was the primary reason. The supply air temperature drop across the evaporator was varied with time at 90% reduced evaporator air flow (Figure 4.2.).

16. The amount of liquid entering the compressor under reduced evaporator air flow conditions was varied from 5 to 20 %. However this quantity was reduced by suction gas superheating which occurred in the compressor shell.

17. The sensible heat ratio (SHR) decreased with reductions in evaporator air flow.

18. Symptoms of low evaporator flow conditions are, large temperature difference across cooling coils, reduced condenser discharge temperatures and reduced superheat and subcooling.

CONCLUSIONS

1. The performance of an air conditioner was not affected up to 50% reduced evaporator air flow conditions. Reductions between 25% and 90% reduced the performance significantly.

2. Return air humidity is an important quantity in the vapor compression cycle and the measured performance. The calibration of RH sensors is also crucial for accurate calculations of capacity and to gain a proper understanding on the role of humidity on performance and temperature measurements.

3. Currently, there is a lack of information on predicting the performance under very low air flow rates. More theoretical and analytical investigations are necessary to improve the understanding on the performance of air conditioners under reduced evaporator air flow rate. In particular the following areas need to be investigated further theoretically; (i.) The overall efficiency of compressor at very low evaporating temperatures and when liquid refrigerant enters the compressor, (ii.) The performance of an evaporator under frosting conditions in the cooling mode.

4. It is necessary to link the degradation of performance factors (Power, Capacity, and EER) with diagnostics to define what is a normal operating conditions of an air conditioner.

5. The temperature measurements were significantly varied with return air humidity. Therefore it is necessary to analyze the role return air humidity on performance to develop a temperature based monitoring device.

6. Many authors (Public Utility Commission of Texas, 1990; Neal, 1986) expressed the concern that the use of large evaporator coils in high SEER equipment's will reduce the dehumidifying capacity of the evaporator coil. The same concern was also expressed when indicating the installation of oversized coils. However, from the Psychrometric chart (Figures A.2

to A.10) we can see that the SHR decrease with reduction in evaporator air flow for the constant area expansion tube. From the cited literature's in Chapter 2, we can recognize that reduced evaporator air flow situations are common in residential cooling systems. Under these conditions employing larger size coils may not be a problem regarding dehumidification. This is a tentative conclusion and more study should be made on this topic.

7. As air flow across evaporator was reduced the power consumption was reduced by 5 to 21%. This may imply that as utilities fix degraded air conditioners the demand may go up by 5 to 21% while usage goes down (i.e. the EER will increase).

FUTURE DIRECTIONS

The preliminary results from the first phase of this on-going project are encouraging. Experience with degraded tests can provide a better procedure to simulate degradations in the future. The ultimate goal of this project is to develop a temperature based monitoring and diagnostics procedure. Experience with preliminary tests indicated that easily identifiable temperature patterns exist for reduced evaporator air flow which can be utilized for developing an automated monitoring procedure (Figures 5.5, 5.6, and 5.7).

An important conclusion which emerges from the test bench results is return air humidity is an important quantity in predicting the performance and temperature measurements. The difficulties arise in calibration of RH sensors is discussed in the calibration section. Therefore, it is necessary to develop normalized or non-dimensional temperature ratios which can predict the performance under varying return air humidity conditions. It is also imperative to develop a model which can predict the performance under degraded conditions. The two key areas which need to be developed further theoretically and quantitatively are, 1. The heat transfer characteristics of a frost covered evaporator coil, 2. Performance and efficiency characteristics of a compressor when liquid refrigerant start entering the compressor.

ACKNOWLEDGMENTS

This work was funded through the Texas A&M Energy Systems Laboratory Research Consortium.

REFERENCES

Air: Psychrometric Calculations. (1991). Energy Systems Laboratory, Mechanical Engineering Department, Texas A&M University.

American Society of Heating Refrigeration and Air Conditioning Engineers. (1985). Laboratory Methods of testing Fans for rating. (ANSI/ASHRAE Standard 51-1985). Atlanta.

American Society of Heating Refrigeration and Air Conditioning Engineers. (1983). Methods of testing Seasonal efficiency of Unitary Air Conditioners and Heat pumps. (ASHRAE Standard 116-1983). Atlanta.

Anderson, R. T.; & Neri, L. (1990). Reliability-Centered maintenance, Management and Engineering methods. New York: Elsevier Applied Science Publications.

Bryant, J. A. & O'Neal, D. L. (1992). Calibration of Relative Humidity Transducers for Use in the Texas LoanSTAR Program. Proceedings of the Eighth Symposium on Improving Building Systems in Hot and Humid Climates (pp. 229-233). Dallas, TX: Energy Systems Laboratory, Mechanical Engineering Department, Texas A&M University.

CoolGuard, Electronic Monitoring System. (1992). Dencor Inc., Denver, Colorado.

Danfoss-EMC Inc., Fort Myers, Florida.

Duffy, G. (1991, April 1). 1991 Statistical Panorama. Air Conditioning Heating and Refrigeration News.

Educational Facilities Laboratories. (1978). The Economy of Energy Conservation in Educational Facilities (2nd ed.). New York, EFL.

Energy Information Administration. (1989). Household Energy Consumption and Expenditures 1987. DOE/EIA-0321/1(87). Washington, DC: U.S. Government Printing Office.

Energy Information Administration. (June 1990). Monthly Energy Review. Washington, DC: U.S. Government Printing Office.

Energy Prices Continue to Edge Upward. (1991, April 8). Air Conditioning Heating and Refrigeration News.

Farzad, M.(1990). Modeling the effects of refrigerant charging on air conditioner performance characteristics for three expansion devices. Ph. D. Dissertation, Mechanical Engineering Department, Texas A&M University, Texas.

Fluke (Trademark). (1992). Trouble shooting guide, HVAC&R systems, Service tips with Fluke thermometers and multimeters. John Fluke Mfg. Co., Inc., 1992.

Foster, G. (March 1992). An electronic crystal ball for service men. Refrigeration and Air Conditioning (U.K.).

Haberl, J., Kissock, K., Belur, R., Sparks, R. (Proposed for ASME, 1993, Washington, D.C.). Improving the Paradigm for Displaying Complex Building Energy Consumption Data.

Hawken, P. J., Hearty, P. F., & Lemal, C. (1989). The Influence of Two-Phase Flow on a Coriolis Effect Mass Flow Meter. ASHRAE Transactions, pp. 310-323.

Hewett, J. M., Bohac, D. L., Landry, R. W., Dunsworth, T. S., Englander, S. L., & Peterson, G. A. (1992). Measured energy and demand impacts on efficiency tune-ups for small commercial cooling systems. In Anderson, R., & Haberl, J. (Eds.), Proceedings of the ACEEE 1992 Summer Study on Energy Efficiency in Buildings (Vol. 3, pp 3.131-3.145). Washington, DC: ACEEE.

Houcek, J.; & Thedford, M.; (1984). A Research in to a New Method of Refrigeration Charging and the Effects of Improper Charging. Proceedings of the First Symposium on Improving Building Systems in Hot and Humid Climates (pp. 36-41). Dallas, TX: Energy Systems Laboratory, Mechanical Engineering Department, Texas A&M University.

Kaler, G. M. (1990). Embedded expert system development for monitoring packaged HVAC equipment. ASHRAE Transactions, 96(Pt. 1).

Karger, H.; & Carpenter, C. L. (1978). An analysis of failure patterns of 531 residential air conditioning units. ASHRAE Transactions, 84, (Pt. 2, pp. 462-474).

Kartsounes, G. T., & Erth, R. A. (1971). Computer Calculations of the Thermodynamic properties of Refrigerants 12, 22, and 502. ASHRAE Transactions. pp. 88-103.

Lewis, J. E. (1987). Survey of residential air-to-air heat pump service life and maintenance issues. ASHRAE Transactions, 93(Pt. 2, pp. 1111-1127).

Madison, R. D. (1948). Centrifugal Fans. In Madison (Ed.), Fan Engineering (pp. 215-220). Buffalo, NY: Buffalo forge company.

Mahoney, T. A. (1989, January 30). Six years of growth - it can be sustained to end of decade. Air Conditioning Heating and Refrigeration News.

Mahoney, T. A. (1992, June 22). No surprises in proposed rule. Air Conditioning Heating and Refrigeration News.

National Bureau of Standards (Currently NIST). (1983). General guidelines for the on-site calibration of humidity and misture control systems in buildings. Building Science Series, No. 157. U.S. Department of Commerce, National Bureau of Standards. Washington, DC.

National Bureau of Standards. (1983). Computer modeling of the vapor compression cycle with constant flow area expansion device. Building Science Series, No. 155. U.S. Department of Commerce, National Bureau of Standards. Washington, DC.

Neal, C. L. (1986). Efficiency in Real Life Residential Air Conditioners, (Staff rep. AEC-R-87-3). North Carolina Alternative Energy Corporation. Rayleigh, NC.

Neal, C. L. (1987, October). Real Life Residential Air Conditioning. Refrigeration Service and Contracting. pp. 24-27.

Oak-Ridge National Laboratories. (1981). A steady state computer design model for Air-to-Air heat pumps, (ORNL/CON-80). Energy division, ORNL, Oak Ridge, TN.

Powell, P. (1988, May). Healthy debate or signs of confusion. Refrigeration Service and Contracting. p. 18.

Proctor, J. (1991). Pacific Gas and Electric Appliance Doctor Pilot Project. Proctor Engineering Group, San Francisco, CA.

Public Utility Commission of Texas, (PUCT). (1990). Interim Report for the PUCT End-Use Modeling Project. Public Utility Commission of Texas, Electric Division.

Public Utility Commission of Texas, (PUCT). (1990). Final Report for Phase-3 of the PUCT End-Use Modeling Project. Public Utility Commission of Texas, Electric Division.

Reddy, T. A.; Vaidya, S., Griffith, L., Bhattacharyya, S., & Claridge, D. E. (1992). A field study on residential air-conditioning peak loads during summer in College Station, Texas. Energy Systems Laboratory, Mechanical Engineering Department, Texas A&M University, College Station, Texas.

Rutkowski, H.; & Healy, J. H. (1990). Selecting Residential Air-Cooled Cooling Equipment based on Sensible and Latent Performance. ASHRAE Transactions. pp. 851-855.

Silver, T. (1989, December). Training for the Future. Contracting Business. pp. 153-154.

Texas Governor's Energy Office. (1990). Save you district thousands of dollars in unnecessary utility costs, Energy efficient school design program. Governor's Energy Office, Texas.

Threlkeld, J. (1970). Thermal Environmental Engineering, (2nd ed.). pp. 62-63. Prentice-Hall, NY.

Tree, R. D.; & Lamb, G. D. (1981). DOE test procedure setup measurement errors for Unitary air conditioners, Part 1: ASHRAE Transactions,.87(Pt. 2).

United States Government Public Law 100-12-March 17, 1987. (1987). National Appliance Energy Conservation Act of 1987. Washington, DC. U. S. Government Documents.

United States Government. (1979, December 27). Test Procedures for Central Air Conditioners, Including Heat Pumps. Federal Register, 44. No. 249, .pp. 76700-76723.

Wheeler, J. (1989, April). Troubleshooting by touch. Contracting Business.

Wheeler, J. (1991, October). How not to Charge Systems. Contracting Business. pp. 60-61.

Zarnikau, J.; Hunn, B., Baughman, M., Nichols, S., Gandhi, U., Bullock, D., & Wang, X. (1992). Opportunities for energy efficiency in Texas. Phase 1: Preliminary estimates of potential savings. Center for Energy Studies, The University of Texas at Austin, TX.

APPENDIX

DATA ACQUISITION AND ANALYSIS

A detailed review of data acquisition and analysis is discussed here. The time series plots for standard and degraded tests were presented exactly as it was measured except the outdoor unit power consumption (Figure 4.1 and 4.2). Up to 50% reductions in evaporator air flow a blower in the Psychrometric room indoor section was used by varying the damper outlet and using the flow restrictor. However it was difficult to obtain a very low air flow rates (300 CFM and 125 CFM) using this blower, therefore the blower which was mounted on the test bench was used to maintain the air flow across the evaporator. The watt transducer which was used to measure the power was measuring the total power consumed by the test bench. Therefore, for 75% and 90% case the power consumption measured included the blower power consumption. After the completion of all the degraded tests, the blower mounted on the test bench alone was operated and the power consumption for maintaining the supply air flow rate of 300 CFM and 120 CFM were measured. This quantity was deducted from the total power measurement to obtain the outdoor unit power consumption.

Relative humidity values are presented as measured. During the performance calculations these values are adjusted with the calibration results of RH sensors. Airflow across evaporator was reduced when dehumidification started occurring at the surface of evaporator. This caused a small variation in power and air flow rate. Equilibrium conditions during 75% reduced evaporator air flow was achieved slowly and during 90% reduced evaporator air flow rate the steady state conditions were never obtained.

The measurement of mass flow rate during the 90% reduced air flow rate was erratic due to the presence of vapor in the liquid line. This error was minimized by employing a small capacity mass flow sensor. An approximate path of the data acquisition and analysis is shown in Figure A.1 in the following page.

		Low RH (20%)			Medium RH (45%)			High RH (65%)		
		Power	Capacity	EER	Power	Capacity	EER	Power	Capacity	EER
70 F Outdoor	Standard	0.00	0.00	0.00	0.00	0.00	0.00	0.00	0.00	0.00
	25% reduction	-9.59	-0.77	9.75	-2.46	0.35	2.88	-5.78	-3.08	2.86
	50% reduction	-13.12	-21.42	-9.55	-6.98	-11.96	-5.35	-14.41	-15.03	-0.72
	75% reduction	-15.96	-28.15	-14.50	-10.47	-21.64	-12.47	-17.22	-21.63	-5.33
	90% reduction	-22.40	-50.41	-36.10	-15.56	-33.26	-20.96	-19.70	-47.98	-35.22
85 F Outdoor	Standard	0.00	0.00	0.00	0.00	-0.00	0.00	0.00	0.00	0.00
	25% reduction	-6.37	-2.91	3.70	-4.49	-1.11	3.54	-5.43	-3.42	2.13
	50% reduction	-11.05	-25.73	-16.51	-9.55	-20.97	-12.63	-12.94	-19.56	-7.61
	75% reduction	-14.90	-34.05	-22.51	-13.74	-33.31	-22.68	-16.12	-25.89	-11.66
	90% reduction	-24.98	-61.69	-48.94	-18.38	-39.10	-25.39	-21.94	-45.48	-30.15
100 F Outdoor	Standard	0.00	-4.80	-4.80	0.00	0.00	0.00	0.00	0.00	0.00
	25% reduction	-7.98	-7.90	0.10	-3.66	-2.46	1.24	-4.83	-3.45	1.45
	50% reduction	-14.32	-31.92	-20.54	-11.18	-21.82	-11.98	-10.68	-18.98	-9.30
	75% reduction	-18.23	-43.87	-31.35	-13.23	-31.40	-20.94	-15.04	-28.57	-15.93
	90% reduction	-25.61	-81.07	-74.56	-20.09	-45.67	-32.01	-22.93	-41.03	-23.49

Table A.1. Summary of reduction in performance (refrigerant side)

		Low RH (20%)			Medium RH (45%)			High RH (65%)		
		Power	Capacity	EER	Power	Capacity	EER	Power	Capacity	EER
70 F Outdoor	Standard	2970	32537	10.96	2807	32830	11.70	2982	35279	11.83
	25% reduction	2685	32286	12.02	2738	32946	12.03	2810	34191	12.17
	50% reduction	2580	25567	9.91	2611	28903	11.07	2552	29977	11.75
	75% reduction	2496	23379	9.37	2513	25726	10.24	2469	27648	11.20
	90% reduction	2305	16135	7.00	2370	21911	9.24	2395	18352	7.66
85 F Outdoor	Standard	3227	31005	9.61	3228	32844	10.17	3313	35588	10.74
	25% reduction	3021	30737	10.17	3083	32480	10.53	3133	34372	10.97
	50% reduction	2870	23510	8.19	2920	25956	8.89	2884	28626	9.92
	75% reduction	2746	20878	7.60	2784	21904	7.87	2779	26373	9.49
	90% reduction	2421	12127	5.01	2635	20002	7.59	2586	19403	7.50
100 F Outdoor	Standard	3605	29797	8.27	3577	31004	8.67	3685	34124	9.26
	25% reduction	3317	28829	8.69	3446	30241	8.78	3507	32945	9.39
	50% reduction	3089	21310	6.90	3177	24238	7.63	3292	27646	8.40
	75% reduction	2948	17569	5.96	3104	21268	6.85	3131	24374	7.79
	90% reduction	2682	5925	2.21	2858	16844	5.89	2840	20123	7.09

Low RH: Return 80 F DBT, 20% RH
Med RH: Return 80 F DBT, 45% RH
High RH: Return 80 F DBT, 65% RH

Power : Total power (Blower + OD Unit), Watts
Capacity: Refrigerant side capacity (BTUH)
EER : (Capacity / Power)

Table A.2. Summary of electric demand, cooling capacity, and EER (refrigerant side)

	List of Temperature Difference	Standard Test (DEG F)	Reduced air flow Degraded tests			
			25% reduction (DEG F)	50% reduction (DEG F)	75% reduction (DEG F)	90% reduction (DEG F)
Low RH (20%)						
70 F Outdoor	1. Supply air temperature drop	25.8	29.9	34.1	45.0	52.6
	2. Condenser air temperature rise	15.3	14.1	12.4	12.0	9.0
	3. Ref superheat at suction	10.2	15.2	0.0	0.0	0.0
	4. Ref Subcool at liquid line	9.6	8.5	6.9	6.6	4.3
85 F Outdoor	1. Supply air temperature drop	24.8	27.7	32.1	41.6	51.1
	2. Condenser air temperature rise	15.6	14.3	12.0	12.0	8.8
	3. Ref superheat at suction	0.0	0.0	0.0	0.0	0.0
	4. Ref Subcool at liquid line	8.5	5.8	5.5	6.0	4.1
100 F Outdoor	1. Supply air temperature drop	23.9	25.9	30.3	38.3	46.8
	2. Condenser air temperature rise	16.2	14.5	11.7	10.1	8.7
	3. Ref superheat at suction	0.0	0.0	0.0	0.0	0.0
	4. Ref Subcool at liquid line	6.6	5.0	4.5	3.7	4.0
Med RH (45%)						
70 F Outdoor	1. Supply air temperature drop	20.1	23.2	26.6	38.2	46.0
	2. Condenser air temperature rise	13.3	17.3	13.9	14.9	12.5
	3. Ref superheat at suction	38.6	33.2	3.4	0.0	0.0
	4. Ref Subcool at liquid line	11.3	12.7	9.7	8.9	4.3
85 F Outdoor	1. Supply air temperature drop	20.1	23.2	26.0	33.7	41.5
	2. Condenser air temperature rise	16.4	18.0	14.9	14.5	13.4
	3. Ref superheat at suction	21.6	17.5	0.0	0.0	0.0
	4. Ref Subcool at liquid line	11.8	11.0	7.3	7.8	4.2
100 F Outdoor	1. Supply air temperature drop	19.5	22.5	24.5	34.0	39.8
	2. Condenser air temperature rise	16.9	18.9	15.1	16.5	13.4
	3. Ref superheat at suction	3.7	0.0	0.0	0.0	0.0
	4. Ref Subcool at liquid line	10.1	10.6	6.9	8.9	3.2
High RH (65%)						
70 F Outdoor	1. Supply air temperature drop	17.5	18.4	25.0	33.7	31.8
	2. Condenser air temperature rise	16.5	17.7	15.8	15.0	10.7
	3. Ref superheat at suction	36.4	36.4	15.0	0.0	0.0
	4. Ref Subcool at liquid line	13.4	13.7	11.9	8.9	5.2
85 F Outdoor	1. Supply air temperature drop	16.9	18.0	23.4	32.1	34.1
	2. Condenser air temperature rise	16.9	18.4	16.1	15.1	10.5
	3. Ref superheat at suction	26.7	28.2	0.0	0.0	0.0
	4. Ref Subcool at liquid line	11.8	12.3	9.6	7.9	4.3
100 F Outdoor	1. Supply air temperature drop	16.8	17.1	21.4	31.1	37.4
	2. Condenser air temperature rise	17.2	18.4	16.4	15.4	12.9
	3. Ref superheat at suction	17.3	17.9	0.0	0.0	0.0
	4. Ref Subcool at liquid line	9.9	10.5	8.3	7.4	3.1

Table A.3. Summary of temperature measurements

	First part of the degraded test				Last part of the degraded test			
	Medium RH			High RH	Medium RH			High RH
Outdoor temp.	70 F	85 F	100 F	100 F	70 F	85 F	100 F	100 F
Return air (DBT/RH)	80.4 F/50.6%	80 F/50.2%	80.4 F/49.8%	80.8 F/69%	80.7 F/50.2%	80.5 F/50%	79.5 F/49.8%	81F/66%
Supply air (DBT/RH)	34 F/77%	38 F/85%	41 F/85%	43 F/86%	55 F/89 %	57 F/86%	59 F/85%	50 F/94%
Air flow (CFM)	118	117	118	117	100	101	102	112
Ref. flow (lb/min)	5.45	5.5	5.2	5.71	2.33	2.22	2.11	4.57
Power (Watts)	2370	2635	2858	2840	2080	2355	2554	2758
Capacity (Btu/hr)	11781	10175	9793	11701	4754	4226	3464	9118
EER	4.97	3.86	3.43	4.12	2.29	1.79	1.36	3.31

↑ 3 inch.

red 90%. xls.

~~4e7~~ ~~red~~ ~~xls.~~